

Retrieval-Augmented Water Level Forecasting for Everglades

Rahuul Rangaraj^{1*}, Jimeng Shi^{1*}, Rajendra Paudel², Giri Narasimhan¹, Yanzhao Wu¹

¹Florida International University, ²National Park Service, U.S.

{rrang016, jshi008, giri, yawu}@fiu.edu, rajendra_paudel@nps.gov

Abstract

Accurate water level forecasting is crucial for managing ecosystems such as the Everglades, a subtropical wetland vital for flood mitigation, drought management, water resource planning, and biodiversity conservation. While recent advances in deep learning, particularly time series foundation models, have demonstrated success in general-domain forecasting, their application in hydrology remains underexplored. Furthermore, they often struggle to generalize across diverse unseen datasets and domains, due to the lack of effective mechanisms for adaptation. To address this gap, we introduce Retrieval-Augmented Forecasting (RAF) into the hydrology domain, proposing a framework that retrieves historically analogous multivariate hydrological episodes to enrich the model input before forecasting. By maintaining an external archive of past observations, RAF identifies and incorporates relevant patterns from historical data, thereby enhancing contextual awareness and predictive accuracy without requiring the model for task-specific retraining or fine-tuning. Furthermore, we explore and compare both *similarity-based* and *mutual information-based* RAF methods. We conduct a comprehensive evaluation on real-world data from the Everglades, demonstrating that the RAF framework yields substantial improvements in water level forecasting accuracy. This study highlights the potential of RAF approaches in environmental hydrology and paves the way for broader adoption of adaptive AI methods by domain experts in ecosystem management. The code and data are available at <https://github.com/rahuul2992000/WaterRAF>.

1 Introduction

Everglades is a distinctive subtropical wetland ecosystem, spanning thousands of square miles in South Florida, recognized globally for its critical role in biodiversity conservation, regional flood mitigation, drought management, water resource planning, and sustaining local economies through recreation and infrastructure protection (Paudel et al. 2020). Due to its ecological and socioeconomic significance, accurate water level forecasting is vital for effective management, restoration, and decision-making efforts within the region with profound social impacts (Saberski et al. 2022).

Traditional hydrological models, including physics-based simulations and statistical methods (Pearlstine et al. 2020), have long been used for water level prediction. However,

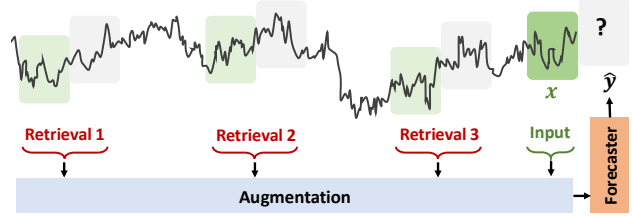


Figure 1: Illustration of retrieval-augmented forecasting (RAF). Previous methods solely consider a lookback window, x , to predict the future, while RAF methods include both x and its retrievals as the augmented input.

these approaches often depend on manually calibrated parameters and fixed assumptions, limiting their flexibility under dynamic or extreme environmental conditions. Recent advancements in deep learning (DL) have shown the potential to learn complex non-linear interactions from data. For example, convolutional neural networks (CNNs), recurrent neural networks (RNNs), and Transformer-based models have achieved remarkable success across diverse time series forecasting tasks (Shi et al. 2025a; Kow et al. 2024; Shi et al. 2025b). Despite the progress, these models need to be re-trained whenever the experimental settings (e.g., different domains) are changed, resulting in domain-specific learning and limited generalization.

More recently, inspired by the transformative success of large language models (LLMs) in natural language processing, time series foundation models (TSFMs) (Miller et al. 2024; Liang et al. 2024) have emerged as powerful forecasting tools. Similar to LLMs, TSFMs are pre-trained on massive and diverse time series datasets and can be adapted to a wide range of downstream tasks through zero-shot inference or lightweight fine-tuning. Notable examples include TimeGPT (Garza and Mergenthaler 2023), TimesFM (Das et al. 2023), and Chronos (Ansari et al. 2024). However, these models rely solely on information from a recent past window, which often contains limited and less informative signals, thereby restricting their predictive capability (Scusolini et al. 2024). It presents unique challenges for hydrological applications, such as water level forecasting in complex river systems, particularly in the face of rare or extreme events. For example, flood events may occur infrequently, providing little signal in immediate history for

*Equal contribution

the model to learn from. Consequently, even the most advanced data-driven models are often ill-equipped to anticipate these low-frequency, high-impact events. To resolve this hurdle, more informative input is needed. From the natural language processing (NLP) field, Retrieval-Augmented Generation (RAG) approaches (Lewis et al. 2020; Fan et al. 2024) have been employed to enhance the model performance by retrieving relevant knowledge from an external database (“context”) and augmenting the query with the retrieved context. Similarly, Retrieval Augmented Forecasting (RAF) methods (Han et al. 2025; Zhang et al. 2025; Yang et al. 2025) have been explored in the time series field, which retrieve contextually relevant time series from a knowledge database and augment the original model input before forecasting. By augmenting the model input with retrieved analogous scenarios, RAF enhances contextual awareness and predictive accuracy. While RAF has shown promising results in various domains, including finance, energy, traffic, and weather (Tire et al. 2024; Liu et al. 2024a), its application to time series forecasting in hydrology, in particular for the Everglades, remains largely underexplored.

In this work, we extended the Retrieval-Augmented Forecasting (RAF) paradigm to hydrological applications, tasked with water level forecasting in the Everglades. The objective is to predict future water levels based on an enriched input of the lookback window. Our approach consists of three key steps: **(1) Retrieval:** Given the current input window, a retriever identifies high-relevance sequences from the knowledge base to serve as relevant contextual information. Both similarity-based and mutual information-based retrieval approaches are explored due to their prevalence and strong performance (Cao et al. 2023; Zhang et al. 2025). **(2) Augmentation:** The retrieved sequences are integrated with the original input to form an augmented input representation. **(3) Forecasting:** This augmented input is then passed to a time series foundation model to generate the water level forecasts. This approach allows forecasting models to access richer temporal context beyond the immediate past window, improving their ability to generalize under dynamic and extreme conditions, without requiring task-specific retraining. This context-driven strategy is especially powerful in data-sparse or non-stationary settings, where statistical properties change over time, opening up a new direction for enhancing water level prediction in hydrologically complex and ecologically sensitive systems. Our contributions are:

- We introduce Retrieval-Augmented Forecasting (RAF) into the hydrology domain, specifically demonstrating its applicability and effectiveness for water level prediction, in the Everglades ecosystem.
- We investigate multiple retrieval mechanisms for identifying historically analogous windows and selecting the most relevant candidates. Moreover, we also examine different augmentation strategies for integrating the retrieved context into the forecasting pipeline.
- Comprehensive experimental results across multiple metrics show that the RAF framework substantially improves water level forecast accuracy, especially for extreme events, outperforming baseline models that solely

rely on the input from the recent past window.

2 Methodology

We first introduce the problem of water level forecasting. Let $\mathbf{X}_{t-l+1:t} \in \mathbb{R}^{l \times m}$ denote a multivariate time series segment with m hydrological variables (e.g., water levels, water flows, rainfall, Potential Evapotranspiration (PET)) observed over a lookback window of length l at timestep t . Given the input \mathbf{X} , the model \mathcal{F} aims to predict the future sequence of water levels, $\mathbf{Y}_{t+1:t+h} \in \mathbb{R}^{h \times n}$, for a horizon of length h at n locations of interest. Formally, it can be formulated as:

$$\mathcal{F}(\mathbf{X}_{t-l+1:t}) \rightarrow \mathbf{Y}_{t+1:t+h}, \quad (1)$$

where the subscripts represent the time range.

In the following, we introduce key components in the proposed RAF framework for water level forecasting, covering the selection of knowledge bases consisting of substantial samples (Section 2.1), retrievers devised to retrieve high-relevance samples from the knowledge base (Section 2.2), augmentation strategies to integrate the retrieved samples with the original input (Section 2.3) and a time series foundation model as the forecaster (Section 2.4).

2.1 Knowledge Base

We briefly discuss the procedure for constructing a knowledge base, i.e., retrieval pool, for RAF. The preprocessing of all multivariate time series in the dataset is performed to construct samples comprising a pair of lookback window and a prediction window, denoted as $(\mathbf{X}_{\text{past}}, \mathbf{Y}_{\text{future}})$. The dataset for the water level prediction tasks is then split chronologically with a ratio of 85% : 15%. Within the RAF framework, the first 85% serves as the knowledge base \mathcal{D} , from which the retriever selects high-relevance samples during the testing phase. The remaining 15% of the samples are used for testing, \mathcal{T} . They are represented as:

$$\mathcal{D} = \left\{ (\mathbf{X}_{\text{past}}^{\text{base}(i)}, \mathbf{Y}_{\text{future}}^{\text{base}(i)}) \right\}_{i=1}^d, \quad (2)$$

$$\mathcal{T} = \left\{ (\mathbf{X}_{\text{past}}^{\text{test}(j)}, \mathbf{Y}_{\text{future}}^{\text{test}(j)}) \right\}_{j=1}^t, \quad (3)$$

where d and t represent the size of the knowledge base and test set, i and j refer to the indices of samples in the knowledge base and the test set.

2.2 Knowledge Retrieval

Relying solely on the original lookback window $\mathbf{X}_{\text{past}}^{(j)} \in \mathbb{R}^{l \times m}$ may be insufficient for accurately forecasting future water levels, $\mathbf{Y}_{\text{future}}^{(j)} \in \mathbb{R}^{h \times n}$, as it provides limited contextual information. Therefore, a retriever is needed to identify a small number of analogous samples to enrich the input of a sole lookback window. To this end, a scoring function is devised to evaluate the similarity or contextualization between the original lookback window $\mathbf{X}_{\text{past}}^{(j)}$ and the candidate lookback windows $\mathbf{X}_{\text{past}}^{(i)}$ from the knowledge base.

$$\text{score} = S(\mathbf{X}_{\text{past}}^{\text{base}(i)}, \mathbf{X}_{\text{past}}^{\text{test}(j)}), \quad (4)$$

where S is the scoring function. In the following, we present two different retrieval methods used in this work.

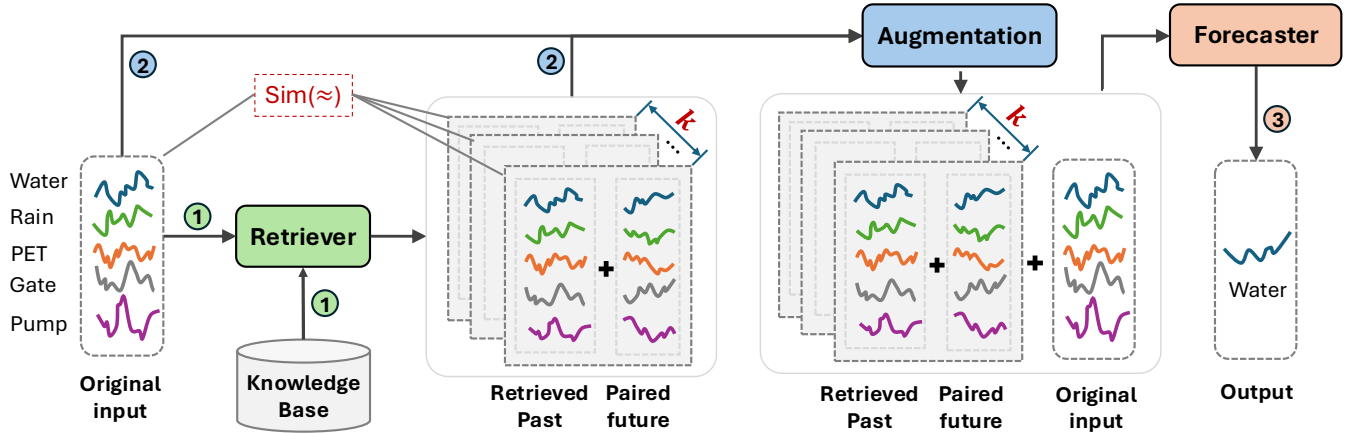


Figure 2: Overview of Retrieval-Augmented Forecasting (RAF) framework for water level forecasting. Given a multivariate hydrological time series, **Retriever** fetches the top- k similar sequences from a knowledge base, based on statistical affinity. The corresponding future observations are also retrieved alongside each context. **Augmentation** component enriches the original input by combining it with the top- k context-future pairs. **Forecaster** takes the augmented input to make the final predictions.

Similarity-based Retriever. It computes the similarity in the embedding space. Following the Chronos work (Ansari et al. 2024), the T5 encoder (Rahman et al. 2020) is employed to encode the lookback window of the original sample (i.e., original input) to an embedding vector with a fixed length, $k = 512$. The same encoding process is applied to all candidate lookback windows from the knowledge base. Then we compute the Euclidean distance between these embedding vectors:

$$\ell_2(\mathbf{e}_{\text{past}}^{\text{base}(i)}, \mathbf{e}_{\text{past}}^{\text{test}(j)}) = \left\| \mathbf{e}_{\text{past}}^{\text{base}(i)} - \mathbf{e}_{\text{past}}^{\text{test}(j)} \right\| \quad (5)$$

Mutual Information-based Retriever. Mutual Information (MI), a fundamental concept from information theory that leans towards entropy, quantifies the statistical dependency between two random variables, capturing both linear and nonlinear relationships. In the context of hydrological forecasting, MI serves as a relevance signal to identify historical contexts most informative about the current system state. The mutual information $MI(\mathbf{X}_{\text{past}}^{\text{base}(i)}, \mathbf{X}_{\text{past}}^{\text{test}(j)})$ is formally defined as:

$$MI = H(\mathbf{X}_{\text{past}}^{\text{base}(i)}) + H(\mathbf{X}_{\text{past}}^{\text{test}(j)}) - H(\mathbf{X}_{\text{past}}^{\text{base}(i)}, \mathbf{X}_{\text{past}}^{\text{test}(j)}), \quad (6)$$

where H denotes the entropy.

Ranking Retrieved Samples. All samples in the knowledge base are ranked based on corresponding scores (e.g., similarity or mutual information), and the top- k highest-scoring samples are retrieved. Each retrieved segment includes a lookback window and its corresponding future window. For clarity, we refer to the retrieved samples as a “context” set,

$$\mathcal{C} = \left\{ (\mathbf{X}_{\text{past}}^{\text{ctx}(z)}, \mathbf{Y}_{\text{future}}^{\text{ctx}(z)}) \right\}_{z=1}^k, \quad (7)$$

where k is the size of context set ($k \ll d$).

2.3 Retrieval Augmentation

To forecast water levels more accurately, the top- k retrieved samples are integrated with the original input to form an augmented input. We explore three augmentation strategies.

Strategy A: Averaging-First, Augmenting-Later. In this approach, we compute the pointwise average over the top- k retrieved candidates, \mathcal{C} , as shown in Eq. (7) by:

$$\bar{\mathbf{C}} = \frac{1}{k} \sum_{z=1}^k \mathcal{C}^{(z)}. \quad (8)$$

Then the averaged context is concatenated with the original input, $\mathbf{X}_{t-l+1:t}$, to form the augmented input: $\mathbf{X}_{\text{aug}} = [\bar{\mathbf{C}}; \mathbf{X}_{t-l+1:t}]$, where “;” denotes temporal concatenation.

Strategy B: Augmenting-First, Averaging-Later. Each candidate in the context set, $\mathcal{C}^{(z)}$, is prepended to the current input individually to form the k augmented inputs $\mathbf{X}_{\text{aug}}^{(z)} = [\mathcal{C}^{(z)}; \mathbf{X}_{t-l+1:t}]$, where $z \in [1, 2, \dots, k]$. The forecaster processes each augmented input individually, generating k predictions that are subsequently averaged for the final forecast.

Strategy C: Long-Context Concatenation. In this approach, all k retrieved contexts are directly concatenated with the current input to form a single augmented input:

$$\mathbf{X}_{\text{aug}} = [\mathbf{C}^{(1)}; \mathbf{C}^{(2)}; \dots; \mathbf{C}^{(k)}; \mathbf{X}_{t-l+1:t}]. \quad (9)$$

2.4 Water Level Forecaster

In this study, we adopt Chronos (Ansari et al. 2024) as the forecasting model due to its strong empirical performance in prior comparative studies on water level prediction tasks (Rangaraj et al. 2025). Nevertheless, our RAF framework is model-agnostic and can be integrated with other pretrained or fine-tuned time series forecasting models. Built on the strong time series foundation model, Chronos, we introduce similarity-based and mutual information-based RAF methods, referred to as Sim-RAF and MI-RAF for brevity.

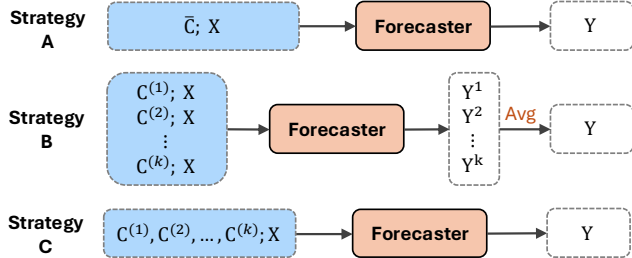


Figure 3: Illustration of three augmentation strategies.

3 Experimental Setup

3.1 Study Area and Dataset

Study Area. The study area focuses on the Everglades National Park, a distinctive subtropical wetland ecosystem vital for ecological balance and socio-economic activities in South Florida (refer to the detailed area map provided in Appendix 8). Within this landscape, we monitored water levels at five key measuring stations, strategically located near major canals, control structures, and natural wetlands. These stations form part of the he Everglades Depth Estimation Network (EDEN) network (Haider et al. 2020) and the South Florida Water Management District’s Environmental Database (DBHYDRO) (South Florida Water Management District 2024), providing high-resolution daily measurements that underpin our forecasting models.

Dataset. Our dataset spans daily records from October 16, 2020, to December 31, 2024, comprising 1538 days and 38 hydrological and meteorological variables. Key inputs considered include rainfall, Potential Evapotranspiration (PET), gate and pump flow, and historical water levels. Data was collected from the Everglades Depth Estimation Network (EDEN) (Haider et al. 2020) and the South Florida Water Management District’s Environmental Database (DBHYDRO) (South Florida Water Management District 2024). The data was split into training, validation, and test sets with an approximate ratio of 85% : 15%. The training set includes data from October 16, 2020, to May 14, 2024, representing 1,307 days, and the test set includes data from May 15, 2024, to December 31, 2024, comprising 231 days.

Task Settings. We ingest the lookback window of 100 days of all 38 variables as input, and forecast water levels at five gauging stations (NP205, P33, G620, NESRS1, NESRS2; see Figure 6 in Appendix 8) over 7, 14, 21, and 28 day horizons. Retrieval-augmented forecasts use a pre-trained Chronos foundation model without fine-tuning.

3.2 Baselines

We consider eight representative baseline methods across two types for the experimental comparison. **(1) Task-specific models:** DLinear (Zeng et al. 2023), TimeMixer (Wang et al. 2024), Kolmogorov-Arnold Networks (KAN) (Liu et al. 2024c) and iTransformer (Liu et al. 2023). **(2) Time series foundation models:** TimeGPT (Garza and Mergenthaler 2023), TimesFM (Das et al. 2023), Timer (Liu et al. 2024b) and Chronos (Ansari et al. 2024).

3.3 Evaluation Metrics

Following the work (Shi et al. 2025b), we used Mean Absolute Error (MAE) (Eq. 10) and Root Mean Squared Error (RMSE) (Eq. 11) to evaluate the overall performance of these models. Additionally, we also include the Symmetric Extremal Dependence Index (SEDI) in (Eq. 12) as a specialized metric for extreme values (Han et al. 2024; Zheng et al. 2025). It classifies each prediction as either “extreme” or “normal” based on upper or lower quantile thresholds. SEDI values belong to the range [0, 1], where higher values indicate better accuracy in identifying extreme water levels.

$$\text{MAE} = \frac{1}{N} \sum_{i=1}^N |y_i - \hat{y}_i|, \text{ and} \quad (10)$$

$$\text{RMSE} = \sqrt{\frac{1}{N} \sum_{i=1}^N (y_i - \hat{y}_i)^2}, \text{ and} \quad (11)$$

$$\text{SEDI}(p) = \frac{\Sigma(\hat{y} < y_{\text{low}}^p \& y < y_{\text{low}}^p) + \Sigma(\hat{y} > y_{\text{up}}^p \& y > y_{\text{up}}^p)}{\Sigma(y < y_{\text{low}}^p) + \Sigma(y > y_{\text{up}}^p)}, \quad (12)$$

where y and \hat{y} denote the ground truth and prediction, respectively. The tests, $\hat{y} > y_{\text{up}}^p$ and $y > y_{\text{up}}^p$, determine whether the predicted and observed values are extremes based on the threshold value y_{up}^p . Following the work (Han et al. 2024), we set 10% and 90% as the low and high thresholds, respectively. N is the number of samples.

3.4 Implementation Details

For task-specific models, we first train them before conducting the evaluation. The training is performed for a total of 1,000 epochs, starting with a learning rate of $1e^{-3}$. We used a batch size of 32 for training, and early stopping is executed if the training loss does not decrease for 50 iterations. For pre-trained time series foundation models, we directly used their existing model weights for inference on our test set. For our retrieval-augmented forecasting approaches, a strong time series foundation, Chronos, is utilized as the forecaster. All experiments were conducted on an NVIDIA A100 GPU with 80GB memory.

4 Results and Analysis

4.1 Overall Comparison with Benchmarks

Table 1 reports the experimental comparison results between our retrieval-augmented forecasting methods, Sim-RAF and MI-RAF, and other representative baseline methods. We highlight three interesting observations. First, Chronos exhibits superiority over other task-specific models and time series foundation models among baselines. Notably, both our Sim-RAF and MI-RAF approaches consistently and significantly outperform this strongest baseline. Second, for the temporal perspective, for short-term water level forecasting (lead time of 7 days), Sim-RAF yields an MAE and RMSE improvements by 4.1% and 5.1%, respectively, while MI-RAF boosts the performance by 2.7% and 3.6%, compared to Chronos. Our methods show even higher improvements for long-term prediction: Sim-RAF presents an

Models	Lead Time	NP205		P33		G620		NESRS1		NESRS2		Overall	
		MAE	RMSE										
DLinear (Zeng et al. 2023)	7	0.140	0.235	0.087	0.129	0.097	0.148	0.101	0.145	0.101	0.142	0.105	0.160
	14	0.203	0.320	0.123	0.168	0.144	0.199	0.144	0.192	0.146	0.191	0.152	0.214
	21	0.305	0.416	0.246	0.282	0.266	0.316	0.277	0.319	0.277	0.317	0.274	0.330
	28	0.375	0.481	0.317	0.353	0.338	0.388	0.351	0.392	0.352	0.390	0.347	0.401
TimeMixer (Wang et al. 2024)	7	0.181	0.309	0.077	0.124	0.095	0.150	0.077	0.129	0.076	0.133	0.102	0.169
	14	0.249	0.358	0.125	0.168	0.160	0.200	0.109	0.160	0.110	0.163	0.151	0.210
	21	0.449	0.523	0.182	0.222	0.240	0.288	0.176	0.216	0.170	0.214	0.244	0.293
	28	0.512	0.610	0.218	0.265	0.302	0.351	0.206	0.249	0.191	0.238	0.286	0.343
KAN (Liu et al. 2024c)	7	0.176	0.268	0.085	0.131	0.101	0.146	0.076	0.130	0.071	0.123	0.102	0.160
	14	0.257	0.374	0.126	0.169	0.148	0.203	0.116	0.168	0.110	0.165	0.151	0.216
	21	0.292	0.441	0.144	0.196	0.160	0.225	0.138	0.200	0.133	0.199	0.174	0.252
	28	0.357	0.502	0.165	0.216	0.188	0.258	0.185	0.243	0.178	0.240	0.214	0.292
iTransformer (Liu et al. 2023)	7	0.205	0.320	0.080	0.120	0.083	0.135	0.072	0.118	0.070	0.111	0.102	0.161
	14	0.282	0.416	0.121	0.165	0.131	0.184	0.113	0.161	0.105	0.150	0.150	0.215
	21	0.310	0.455	0.127	0.175	0.154	0.212	0.129	0.178	0.123	0.171	0.169	0.238
	28	0.335	0.503	0.156	0.206	0.193	0.263	0.160	0.215	0.144	0.201	0.198	0.278
TimeGPT (Garza and Mergenthaler 2023)	7	0.162	0.268	0.090	0.163	0.104	0.189	0.097	0.183	0.098	0.182	0.110	0.197
	14	0.209	0.349	0.112	0.187	0.130	0.216	0.112	0.198	0.107	0.198	0.134	0.230
	21	0.275	0.366	0.160	0.241	0.213	0.316	0.152	0.235	0.148	0.234	0.190	0.279
	28	0.399	0.498	0.241	0.325	0.280	0.407	0.220	0.304	0.222	0.315	0.273	0.370
TimesFM (Das et al. 2023)	7	0.191	0.316	0.093	0.149	0.099	0.169	0.096	0.166	0.083	0.149	0.133	0.190
	14	0.372	0.561	0.176	0.242	0.169	0.250	0.150	0.225	0.143	0.216	0.202	0.299
	21	0.535	0.741	0.239	0.306	0.230	0.312	0.198	0.271	0.194	0.272	0.279	0.380
	28	0.684	0.893	0.288	0.348	0.299	0.366	0.236	0.307	0.235	0.317	0.348	0.446
Timer (Liu et al. 2024b)	7	0.258	0.342	0.129	0.172	0.148	0.203	0.122	0.169	0.114	0.161	0.154	0.209
	14	0.442	0.556	0.220	0.259	0.269	0.320	0.199	0.241	0.186	0.230	0.263	0.321
	21	0.574	0.696	0.275	0.314	0.362	0.410	0.250	0.290	0.226	0.269	0.338	0.396
	28	0.650	0.775	0.309	0.354	0.429	0.481	0.279	0.320	0.250	0.292	0.383	0.444
Chronos (Ansari et al. 2024)	7	0.125	0.224	0.058	0.107	0.065	0.124	0.065	0.124	0.058	0.112	0.074	0.138
	14	0.198	0.343	0.095	0.156	0.103	0.179	0.099	0.172	0.086	0.158	0.116	0.202
	21	0.271	0.454	0.133	0.204	0.145	0.231	0.135	0.217	0.116	0.210	0.160	0.261
	28	0.337	0.536	0.168	0.249	0.186	0.280	0.169	0.257	0.141	0.232	0.200	0.311
Sim-RAF (Our method)	7	0.116	0.208	0.055	0.103	0.066	0.125	0.061	0.115	0.057	0.107	0.071	0.131
	14	0.188	0.331	0.088	0.148	0.101	0.178	0.091	0.160	0.087	0.160	0.111	0.194
	21	0.253	0.430	0.117	0.185	0.138	0.229	0.122	0.198	0.117	0.210	0.150	0.247
	28	0.320	0.512	0.146	0.222	0.173	0.276	0.148	0.230	0.142	0.224	0.186	0.293
MI-RAF (Our method)	7	0.119	0.211	0.055	0.103	0.066	0.125	0.062	0.117	0.058	0.111	0.072	0.133
	14	0.181	0.325	0.084	0.146	0.098	0.177	0.091	0.160	0.084	0.156	0.107	0.193
	21	0.241	0.428	0.112	0.182	0.130	0.224	0.116	0.195	0.109	0.192	0.142	0.244
	28	0.297	0.509	0.136	0.215	0.165	0.271	0.138	0.225	0.128	0.218	0.173	0.288

Table 1: Performance across 5 stations (NP205, P33, G620, NESRS1, NESRS2) for lead times of 7, 14, 21, and 28 days. The first four baseline models are task-specific, followed by four pre-trained time series foundation models. The last two are our RAF methods with similarity-based and mutual information-based implementations. The best results are in **bold**.

MAE and RMSE improvements by 7.0% and 5.8%, respectively, while MI-RAF enhances the performance by 13.5% and 7.4%. These results collectively underscore the power and potential of retrieval-augmented water level forecasting. Last but not least, the performance of all models varies across the spatial locations, with the worst scenarios for the NP205 station. A possible reason for the lower performance at the NP205 station is its weaker correlation with other water stations (see Figure 7 in Appendix B). This suggests that dedicated domain knowledge is still needed to enhance the performance for particular stations.

4.2 Study on Extreme Events

It is critical to study the model’s performance on extreme cases. Following the work (Han et al. 2024), we use the SEDI metric to evaluate model performance under extreme events and report the results in Tables 2 and 3. The obser-

vations are as follows. Compared to the strongest baseline, Sim-RAF and MI-RAF present an overall improvement by 4.4% and 2.7% for the predictions with a lead time of 7 days. and exhibit an overall improvement by 14.1% and 8.4%, for the predictions with a lead time of 28 days. These results show that both of our RAF approaches significantly outperform other baseline models, demonstrating the superiority of RAF-based methods for extreme values forecasting, in particular for the longer lead time prediction.

4.3 Effect of Retrieval Database Size

To investigate the effect of the size of the retrieval pool, we compute mean absolute error (MAE) for five levels of retrieval pool sizes to cover 0%, 25%, 45%, 65%, and 85% of the entire knowledge base across different lead times (7, 14, 21, and 28 days) in Figure 4. We first observe that the 0% retrieval coverage corresponds to the Chronos model without

Models	NP205	P33	G620	NESRS1	NESRS2	Overall
DLinear	0.475	0.456	0.456	0.523	0.478	0.477
TimeMixer	0.642	0.512	0.731	0.682	0.714	0.656
TimeGPT	0.300	0.217	0.152	0.095	0.086	0.170
TimesFM	0.550	0.043	0.065	0.119	0.086	0.172
Chronos	0.717	0.696	0.755	0.651	0.690	0.702
Sim-RAF	0.760	0.739	0.755	0.697	0.714	0.733
MI-RAF	0.739	0.717	0.755	0.674	0.714	0.720

Table 2: SEDI values (the higher, the better) for predicting extreme values across 5 stations with a lead time of 7 days. The best results are in **bold**.

Models	NP205	P33	G620	NESRS1	NESRS2	Overall
DLinear	0.500	0.369	0.369	0.352	0.113	0.394
TimeMixer	0.119	0.049	0.341	0.000	0.000	0.102
TimeGPT	0.173	0.217	0.152	0.095	0.086	0.144
TimesFM	0.152	0.043	0.065	0.119	0.086	0.093
Chronos	0.619	0.738	0.525	0.425	0.131	0.488
Sim-RAF	0.690	0.738	0.775	0.425	0.158	0.557
MI-RAF	0.690	0.690	0.525	0.450	0.289	0.529

Table 3: SEDI values (the higher, the better) for predicting extreme values across 5 stations with a lead time of 28 days. The best results are in **bold**.

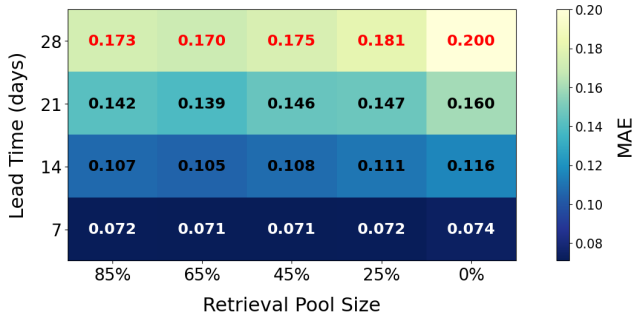


Figure 4: Performance (MAE) vs. Retrieval Pool Size.

retrieval augmentation, which performs worst overall, especially at longer horizons. This again verifies the effectiveness and necessity of retrieval-augmented forecasting. More interestingly, we also noticed the MAEs decrease as the retrieval pool size increases when the coverage is less than 65%, which reveals that a larger retrieval pool can result in retrieving more contextual samples and benefit the subsequent water level forecasting tasks. However, the performance drops slightly when the coverage reaches 85%. The possible reason is that the too large size of the retrieval pool may introduce noisy time series samples, increasing the retrieval difficulty and diluting the usefulness of retrieved contexts. A comprehensive justification for this observation is deferred to future work.

Overall, these results empirically validate that retrieving relevant time series from a knowledge base significantly enhances predictive accuracy, particularly in long-range water level forecasting tasks. Additionally, the size of this retrieval base requires careful selection due to its substantial impact.

5 Visualizations

For the intuitive insights, we visualize the ground truth and predicted water levels in Figure 5. We observed that the Chronos baseline exhibits noticeable deviations from the ground truth, particularly during periods of rapid fluctuation or extreme water levels. In contrast, both Sim-RAF and MI-RAF show predictions that closely track the ground truth, demonstrating the superior accuracy over Chronos. This visual evidence supports our quantitative findings, illustrating how RAF approaches can better capture complex hydrological patterns and improve predictive accuracy. Further visual results can be found in Appendix D.

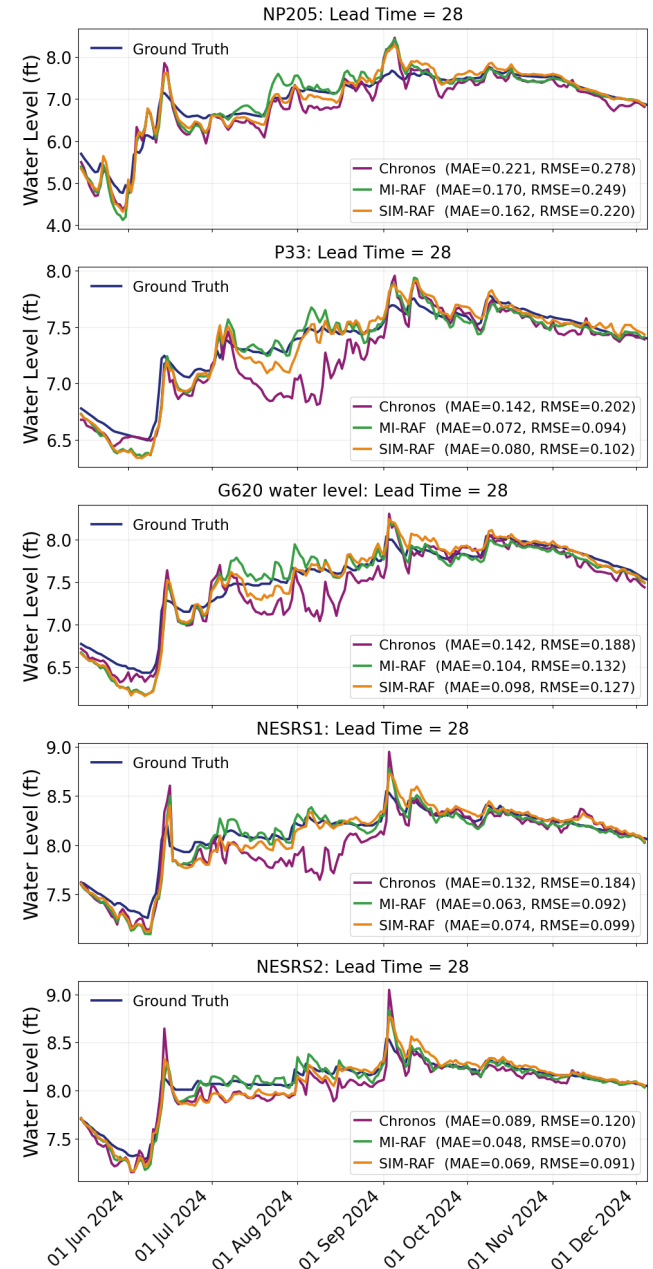


Figure 5: Visualization of true and predicted water levels.

6 Related Work

Physics-based and Statistical Models. Traditional hydrological models, including 1D/2D HEC-RAS ((Muñoz et al. 2022); (Huang and Lee 2023)) and region-specific systems like SFWMM (SFWMD 2005), have been pivotal in simulating water levels across various contexts. While such physics-based models remain foundational, they rely on manually calibrated parameters and static assumptions, limiting their adaptability during anomalous events. Statistical methods, such as Autoregressive Integrated Moving Average (ARIMA) (Agaj et al. 2024) and seasonal ARIMA (SARIMA) (Azad et al. 2022) have proven useful for short-term forecasting and pattern identification. However, their ability to capture complex spatiotemporal dependencies is limited, particularly under extreme variability.

Data-Driven Approaches. Machine learning (ML) models have been largely used in hydrology for streamflow prediction, rainfall-runoff modeling, and groundwater level estimation (Khan and Coulibaly 2006; Nguyen et al. 2021). Despite the progress, they often heavily depend on feature engineering and may struggle with generalization across different basins. Deep learning (DL) stands out by automatically learning relevant features from data. Recurrent Neural Networks (Shi et al. 2023) and Convolutional Neural Networks (Bassah et al. 2025) have been applied to capture sequential and spatial dependencies in hydrological time series of water levels, precipitation, and river discharge (Yin et al. 2025, 2023). The combination of Graph Neural Networks and Transformers (Shi et al. 2025a) has been studied for flood prediction and mitigation in river systems. The above methods are task-specific and need re-training when tasks and domains are changed. More recently, the emergence of time series foundation models (TSFMs) marks a significant paradigm shift to general domains without re-training. These models are pre-trained on massive, diverse time series datasets and can be adapted to downstream tasks with minimal data via zero-shot inference or light fine-tuning. Examples include TimeGPT (Garza and Mergenthaler 2023), TimesFM (Das et al. 2023), Chronos (Ansari et al. 2024), Moment (Goswami et al. 2024), Moirai (Woo et al. 2024), and Timer (Liu et al. 2024b), etc. Recent efforts show the potential of TSFMs on hydrological forecasting (Rangaraj et al. 2025).

Retrieval-Augmented Forecasting. Originating in natural language processing, Retrieval-Augmented Generation (RAG) enhances foundation models by retrieving and incorporating external, contextually relevant data (Lewis et al. 2020). Similar methods have been explored for time series forecasting, referred to as Retrieval-Augmented Forecasting (RAF). For example, RAF (Tire et al. 2024), RATD (Liu et al. 2024a), RAFT (Han et al. 2025), TimeRAF (Zhang et al. 2025), and TimeRAG (Yang et al. 2025) retrieve the relevant data by computing the similarity between the reference and candidate time series from the training set, demonstrating their effectiveness in boosting predictive accuracy. However, the application of RAF to environmental forecasting, particularly in hydrology, remains largely unexplored.

7 Discussion

Compared with conventional forecasting methods that rely solely on a fixed lookback window, our analysis demonstrates that retrieval-augmented forecasting (RAF) provides a significant performance improvement by enriching the constrained temporal context in the input with retrieved time series. With the application of RAF methods to hydrological water level forecasting in the Everglades, we observe substantial performance enhancements, particularly for extended lead times (21 and 28 days) and extreme water levels (defined as values outside the 10th and 90th percentile ranges). The enhanced performance can mainly be attributed to the highly relevant retrieved time series samples, which enrich the contextual information available to the model and are crucial for the accurate prediction of these challenging long-term cases and rare events.

While RAF methods enhance overall model performance, spatial variations in forecasting accuracy still exist, indicating a critical need for domain-aware, tailored RAF models. For example, the station NP205 exhibits relatively lower performance, likely due to its unique geographical location and characteristics. In such cases, constructing a knowledge base that incorporates a broader spectrum of relevant covariates can be more effective than relying solely on retrieval from historical time series data. Collaboration with domain experts is crucial for determining the relevant covariates.

Furthermore, we examined the impact of varying the retrieval pool size on water level forecasting. Although larger retrieval pools generally improve performance, the optimal size requires careful selection, as overly large pools can introduce noise and impair forecasting accuracy.

8 Conclusions

In this paper, we explore both similarity-based and mutual information-based retrieval-augmented forecasting (RAF) methods for water level prediction in the Everglades. By identifying and leveraging historically relevant hydrological patterns from a knowledge base, our RAF framework significantly surpasses the conventional models without retrieval, which is particularly effective in challenging scenarios, such as predicting extreme events over long horizons, which often require informative context for more accurate prediction. Overall, our findings underscore the value of combining pre-trained representations with in-domain contextual memory retrieval for hydrological forecasting. Future work can include hybrid retrievers, memory pruning for efficiency, and integration with physically informed models to further advance hydrological forecasting.

Collaboration and Broader Impact

ML and Everglades researchers were involved in multidisciplinary collaborations. Domain experts helped in area selection, data acquisition, data preprocessing, and analysis of the results. This work also helps domain researchers select the best AI models for water level forecasting in the Everglades and provides practical insights for government agencies interested in AI-driven hydrological applications, e.g., flood prediction and management.

References

Agaj, T.; Budka, A.; Janicka, E.; and Bytyqi, V. 2024. Using ARIMA and ETS models for forecasting water level changes for sustainable environmental management. *Scientific Reports*, 14(1): 22444.

Ansari, A. F.; Stella, L.; Turkmen, C.; Zhang, X.; Mercado, P.; Shen, H.; Shchur, O.; Rangapuram, S. S.; Arango, S. P.; Kapoor, S.; et al. 2024. Chronos: Learning the language of time series. *arXiv preprint arXiv:2403.07815*.

Azad, A. S.; Sokkalingam, R.; Daud, H.; Adhikary, S. K.; Khurshid, H.; Mazlan, S. N. A.; and Rabbani, M. B. A. 2022. Water level prediction through hybrid SARIMA and ANN models based on time series analysis: Red hills reservoir case study. *Sustainability*, 14(3): 1843.

Bassah, R.; Corzo, G.; Bhattacharya, B.; Haider, S. M.; Swain, E. D.; and Aumen, N. 2025. Forecasting water levels using the ConvLSTM algorithm in the Everglades, USA. *Journal of Hydrology*, 652: 132195.

Cao, Y.; Zhang, D.; Zheng, X.; Shan, H.; and Zhang, J. 2023. Mutual Information Based Reweighting for Precipitation Nowcasting. In *ICASSP 2023-2023 IEEE International Conference on Acoustics, Speech and Signal Processing (ICASSP)*, 1–5. IEEE.

Das, A.; Kong, W.; Sen, R.; and Zhou, Y. 2023. A decoder-only foundation model for time-series forecasting. *arXiv preprint arXiv:2310.10688*.

Fan, W.; Ding, Y.; Ning, L.; Wang, S.; Li, H.; Yin, D.; Chua, T.-S.; and Li, Q. 2024. A survey on rag meeting llms: Towards retrieval-augmented large language models. In *Proceedings of the 30th ACM SIGKDD conference on knowledge discovery and data mining*, 6491–6501.

Garza, A.; and Mergenthaler, M. 2023. TimeGPT-1. *arXiv preprint arXiv:2310.03589*.

Goswami, M.; Szafer, K.; Choudhry, A.; Cai, Y.; Li, S.; and Dubrawski, A. 2024. Moment: A family of open time-series foundation models. *arXiv preprint arXiv:2402.03885*.

Haider, S.; Swain, E.; Beerens, J.; Petkewich, M. D.; McCloskey, B.; and Henkel, H. 2020. The Everglades depth estimation network (EDEN) surface-water interpolation model, version 3. Technical report, US Geological Survey.

Han, S.; Lee, S.; Cha, M.; Arik, S. O.; and Yoon, J. 2025. Retrieval augmented time series forecasting. *arXiv preprint arXiv:2505.04163*.

Han, T.; Guo, S.; Chen, Z.; Xu, W.; and Bai, L. 2024. WEATHER-5K: A Large-scale Global Station Weather Dataset Towards Comprehensive Time-series Forecasting Benchmark. *arXiv preprint arXiv:2406.14399*.

Huang, P.-C.; and Lee, K. T. 2023. An alternative for predicting real-time water levels of urban drainage systems. *Journal of Environmental Management*, 347: 119099.

Khan, M. S.; and Coulibaly, P. 2006. Application of support vector machine in lake water level prediction. *Journal of Hydrologic Engineering*, 11(3): 199–205.

Kow, P.-Y.; Liou, J.-Y.; Yang, M.-T.; Lee, M.-H.; Chang, L.-C.; and Chang, F.-J. 2024. Advancing climate-resilient flood mitigation: Utilizing transformer-LSTM for water level forecasting at pumping stations. *Science of the Total Environment*, 927: 172246.

Lewis, P.; Perez, E.; Piktus, A.; Petroni, F.; Karpukhin, V.; Goyal, N.; Küttler, H.; Lewis, M.; Yih, W.-t.; Rocktäschel, T.; et al. 2020. Retrieval-augmented generation for knowledge-intensive nlp tasks. *Advances in neural information processing systems*, 33: 9459–9474.

Liang, Y.; Wen, H.; Nie, Y.; Jiang, Y.; Jin, M.; Song, D.; Pan, S.; and Wen, Q. 2024. Foundation models for time series analysis: A tutorial and survey. In *Proceedings of the 30th ACM SIGKDD conference on knowledge discovery and data mining*, 6555–6565.

Liu, J.; Yang, L.; Li, H.; and Hong, S. 2024a. Retrieval-augmented diffusion models for time series forecasting. *Advances in Neural Information Processing Systems*, 37: 2766–2786.

Liu, Y.; Hu, T.; Zhang, H.; Wu, H.; Wang, S.; Ma, L.; and Long, M. 2023. itransformer: Inverted transformers are effective for time series forecasting. *arXiv preprint arXiv:2310.06625*.

Liu, Y.; Zhang, H.; Li, C.; Huang, X.; Wang, J.; and Long, M. 2024b. Timer: Generative Pre-trained Transformers Are Large Time Series Models. In *Forty-first International Conference on Machine Learning*.

Liu, Z.; Wang, Y.; Vaidya, S.; Ruehle, F.; Halverson, J.; Soljačić, M.; Hou, T. Y.; and Tegmark, M. 2024c. Kan: Kolmogorov-arnold networks. *arXiv preprint arXiv:2404.19756*.

Miller, J. A.; Aldosari, M.; Saeed, F.; Barna, N. H.; Rana, S.; Arpinar, I. B.; and Liu, N. 2024. A survey of deep learning and foundation models for time series forecasting. *arXiv preprint arXiv:2401.13912*.

Muñoz, D. F.; Yin, D.; Bakhtyar, R.; Moftakhari, H.; Xue, Z.; Mandli, K.; and Ferreira, C. 2022. Inter-model comparison of Delft3D-FM and 2D HEC-RAS for total water level prediction in coastal to inland transition zones. *JAWRA Journal of the American Water Resources Association*, 58(1): 34–49.

Nguyen, D. H.; Le, X. H.; Heo, J.-Y.; and Bae, D.-H. 2021. Development of an extreme gradient boosting model integrated with evolutionary algorithms for hourly water level prediction. *IEEE Access*, 9: 125853–125867.

Paudel, R.; Van Lent, T.; Naja, G. M.; Khare, Y.; Wiedeholt, R.; and Davis III, S. E. 2020. Assessing the hydrologic response of key restoration components to everglades ecosystem. *Journal of Water Resources Planning and Management*, 146(11): 04020084.

Pearlstine, L. G.; Beerens, J. M.; Reynolds, G.; Haider, S. M.; McKelvy, M.; Suir, K.; Romañach, S. S.; and Nestler, J. H. 2020. Near-term spatial hydrologic forecasting in Everglades, USA for landscape planning and ecological forecasting. *Environmental Modelling & Software*, 132: 104783.

Rahman, W.; Hasan, M. K.; Lee, S.; Zadeh, A.; Mao, C.; Morency, L.-P.; and Hoque, E. 2020. Integrating multimodal

information in large pretrained transformers. In *Proceedings of the conference. Association for computational linguistics. Meeting*, volume 2020, 2359.

Rangaraj, R.; Shi, J.; Shirali, A.; Paudel, R.; Wu, Y.; and Narasimhan, G. 2025. How Effective are Large Time Series Models in Hydrology? A Study on Water Level Forecasting in Everglades. *arXiv preprint arXiv:2505.01415*.

Saberski, E.; Park, J.; Hill, T.; Stabenau, E.; and Sugihara, G. 2022. Improved prediction of managed water flow into Everglades National Park using empirical dynamic modeling. *Journal of Water Resources Planning and Management*, 148(12): 05022009.

Scussolini, P.; Luu, L. N.; Philip, S.; Berghuijs, W. R.; Elander, D.; Aerts, J. C.; Kew, S. F.; van Oldenborgh, G. J.; Toonen, W. H.; Volkholz, J.; et al. 2024. Challenges in the attribution of river flood events. *Wiley Interdisciplinary Reviews: Climate Change*, 15(3): e874.

SFWMD. 2005. Documentation of the south Florida water management model v5.5.

Shi, J.; Myana, R.; Stebliankin, V.; Shirali, A.; and Narasimhan, G. 2023. Explainable parallel rcnn with novel feature representation for time series forecasting. In *International Workshop on Advanced Analytics and Learning on Temporal Data*, 56–75. Springer.

Shi, J.; Yin, Z.; Leon, A.; Obeysekera, J.; and Narasimhan, G. 2025a. FIDLAR: Forecast-Informed Deep Learning Architecture for Flood Mitigation. In *Proceedings of the AAAI Conference on Artificial Intelligence*, volume 39, 28377–28385.

Shi, J.; Yin, Z.; Myana, R. S.; Ishtiaq, K. S.; John, A.; Obeysekera, J.; Leon, A. S.; and Narasimhan, G. 2025b. Deep learning models for water stage predictions in south florida. *Journal of Water Resources Planning and Management*, 151(10): 05025013.

South Florida Water Management District. 2024. DBHYDRO Environmental Database. <https://www.sfwmd.gov/science-data/dbhydro>. [Online; accessed 10-Feb-2025].

Tire, K.; Taga, E. O.; Ildiz, M. E.; and Oymak, S. 2024. Retrieval augmented time series forecasting. *arXiv preprint arXiv:2411.08249*.

Wang, S.; Wu, H.; Shi, X.; Hu, T.; Luo, H.; Ma, L.; Zhang, J. Y.; and Zhou, J. 2024. Timemixer: Decomposable multiscale mixing for time series forecasting. *arXiv preprint arXiv:2405.14616*.

Woo, G.; Liu, C.; Kumar, A.; Xiong, C.; Savarese, S.; and Sahoo, D. 2024. Unified training of universal time series forecasting transformers. *arXiv preprint arXiv:2402.02592*.

Yang, S.; Wang, D.; Zheng, H.; and Jin, R. 2025. Timerag: Boosting llm time series forecasting via retrieval-augmented generation. In *ICASSP 2025-2025 IEEE International Conference on Acoustics, Speech and Signal Processing (ICASSP)*, 1–5. IEEE.

Yin, Z.; Bian, L.; Hu, B.; Shi, J.; and Leon, A. S. 2023. Physic-informed neural network approach coupled with boundary conditions for solving 1D steady shallow water equations for riverine system. In *World Environmental and Water Resources Congress 2023*, 280–288.

Yin, Z.; Shi, J.; Bian, L.; Campbell, W. H.; Zanje, S. R.; Hu, B.; and Leon, A. S. 2025. Physics-informed neural network approach for solving the one-dimensional unsteady shallow-water equations in riverine systems. *Journal of Hydraulic Engineering*, 151(1): 04024060.

Zeng, A.; Chen, M.; Zhang, L.; and Xu, Q. 2023. Are transformers effective for time series forecasting? In *Proceedings of the AAAI conference on artificial intelligence*, volume 37, 11121–11128.

Zhang, H.; Xu, C.; Zhang, Y.-F.; Zhang, Z.; Wang, L.; and Bian, J. 2025. TimeRAF: Retrieval-augmented foundation model for zero-shot time series forecasting. *IEEE Transactions on Knowledge and Data Engineering*.

Zheng, X.; Lin, C.; Chen, S.; Chen, Z.; Shi, J.; Cheng, W.; Obeysekera, J.; Liu, J.; and Luo, D. 2025. SF²Bench: Evaluating Data-Driven Models for Compound Flood Forecasting in South Florida. *arXiv preprint arXiv:2506.04281*.

Reproducibility Checklist

This paper:

- Includes a conceptual outline and/or pseudocode description of AI methods introduced (yes)
- Clearly delineates statements that are opinions, hypothesis, and speculation from objective facts and results (yes)
- Provides well marked pedagogical references for less-familiar readers to gain background necessary to replicate the paper (yes)

Does this paper make theoretical contributions? (no)

If yes, please complete the list below. (answered no)

- All assumptions and restrictions are stated clearly and formally. (yes/partial/no)
- All novel claims are stated formally (e.g., in theorem statements). (yes/partial/no)
- Proofs of all novel claims are included. (yes/partial/no)
- Proof sketches or intuitions are given for complex and/or novel results. (yes/partial/no)
- Appropriate citations to theoretical tools used are given. (yes/partial/no)
- All theoretical claims are demonstrated empirically to hold. (yes/partial/no/NA)
- All experimental code used to eliminate or disprove claims is included. (yes/no/NA)

Does this paper rely on one or more datasets? (yes)

If yes, please complete the list below.

- A motivation is given for why the experiments are conducted on the selected datasets (yes)
- All novel datasets introduced in this paper are included in a data appendix. (yes)
- All novel datasets introduced in this paper will be made publicly available upon publication of the paper with a license that allows free usage for research purposes. (yes)
- All datasets drawn from the existing literature (potentially including authors' own previously published work) are accompanied by appropriate citations. (yes)
- All datasets drawn from the existing literature (potentially including authors' own previously published work) are publicly available. (yes)
- All datasets that are not publicly available are described in detail, with explanation why publicly available alternatives are not scientifically satisfying. (yes)

Does this paper include computational experiments? (yes)

If yes, please complete the list below.

- This paper states the number and range of values tried per (hyper-) parameter during development of the paper, along with the criterion used for selecting the final parameter setting. (yes)
- Any code required for pre-processing data is included in the appendix. (yes).
- All source code required for conducting and analyzing the experiments is included in a code appendix. (yes)

- All source code required for conducting and analyzing the experiments will be made publicly available upon publication of the paper with a license that allows free usage for research purposes. (yes)
- All source code implementing new methods have comments detailing the implementation, with references to the paper where each step comes from (yes)
- If an algorithm depends on randomness, then the method used for setting seeds is described in a way sufficient to allow replication of results. (yes)
- This paper specifies the computing infrastructure used for running experiments (hardware and software), including GPU/CPU models; amount of memory; operating system; names and versions of relevant software libraries and frameworks. (yes)
- This paper formally describes evaluation metrics used and explains the motivation for choosing these metrics. (yes)
- This paper states the number of algorithm runs used to compute each reported result. (yes)
- Analysis of experiments goes beyond single-dimensional summaries of performance (e.g., average; median) to include measures of variation, confidence, or other distributional information. (yes)
- The significance of any improvement or decrease in performance is judged using appropriate statistical tests (e.g., Wilcoxon signed-rank). (yes)
- This paper lists all final (hyper-)parameters used for each model/algorithm in the paper's experiments. (yes)

Appendix

A Study Area and Data Set

A.1 Study Area

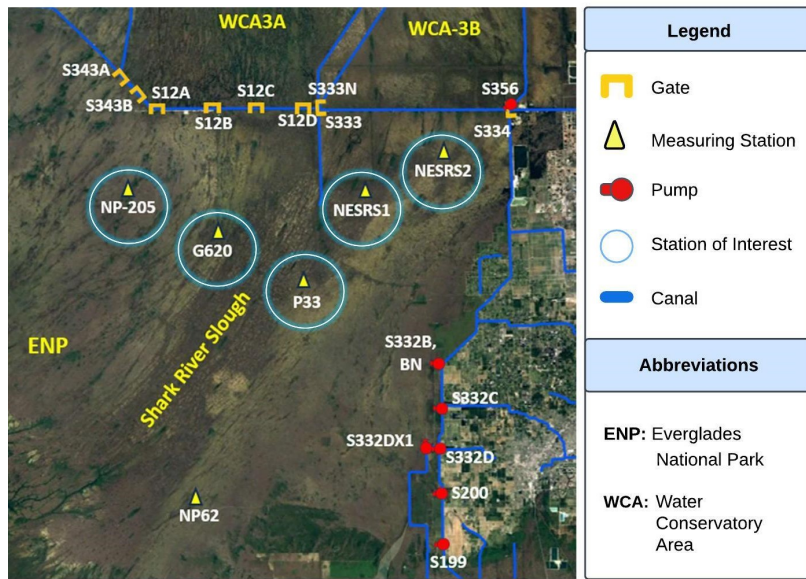


Figure 6: Map of the study area in Everglades National Park, highlighting the hydrological structures and monitoring stations.

A.2 Data summary

Table 4 provides a summary of the key features included in the dataset used for the study. The data encompasses multiple hydrological and meteorological variables collected across various measuring stations. Daily rainfall data, measured in inches, is available for two measuring stations, namely NP205 and P33. Potential Evapotranspiration (PET), measured in millimeters, represents the amount of water that would evaporate and transpire under normal conditions. PET is critical for understanding the water balance in the region as it helps to estimate the loss of water due to evaporation and transpiration. Daily pump and gate flow data is measured in cubic feet per second (cfs). Pumps and gates are used to regulate the water flow between different parts of the Everglades system, making the gate flow data essential for modeling water management operations. Daily water level data, recorded in feet is available for fourteen stations.

Feature	Interval	Unit	#Var.	Location
Rainfall	Daily	inches	2	NP-205, P33
Potential Evapotranspiration	Daily	mm	2	NP-205, P33
Pump flows	Daily	cfs	8	S356, S332B, S332BN, S332C, S332DX1, S332D, S200, S199
Gate flows	Daily	cfs	11	S343A, S343B, S12A, S12B, S12C, S12D, S333N, S333, S334, S344, S18C
Water levels	Daily	ft	14	S12A, S12B, S12C, S12D, S333, S334, NESRS1, NESRS2, NP-205, P33, G620, SWEVER4, TSH, NP62

Table 4: Summary of the dataset.

A.3 Pre-processing

Data Cleaning. The raw water level data was reported in two different vertical datums: the North American Vertical Datum of 1988 (NAVD88) and the National Geodetic Vertical Datum of 1929 (NGVD29). Since direct comparisons require a consistent datum, adjustments were made following domain expert recommendations to standardize all values to NGVD29. For example, the G620 station requires an adjustment of +1.51 ft, while S333T requires +1.54 ft, among others. These values were carefully selected based on the suggestions from domain experts. **Temporal Alignment.** The data pre-processing ensured temporal consistency across all stations. Daily data points were synchronized to a uniform timestamp. **Data Interpolation.** Completeness of data is vital for accurate forecasting of water levels, particularly in ecologically sensitive regions such as the Everglades National Park (ENP). There are certain gates and stations that still exhibit missing values. We employed time-based interpolation and backward fill techniques to address the missing data.

B Correlation Study

To investigate the discrepancy between the NP205 station and other water stations, we compute their correlations. The right plot emphasizes correlations among NP205, P33, G620, NESRS1, and NESRS2, while the left plot extends this analysis to include nearby gates. The results reveal that NP205 exhibits lower correlations with the other stations, with values ranging from 0.76 to 0.85, whereas the remaining stations maintain higher correlations (at least 0.85). This aligns with the spatial distribution shown in Figure 6, where NP205 is positioned separately from the others. The hydrological flow dynamics, influenced by water management structures and natural flow patterns from WCA-3A and WCA-3B to Florida Bay, further explain these variations.

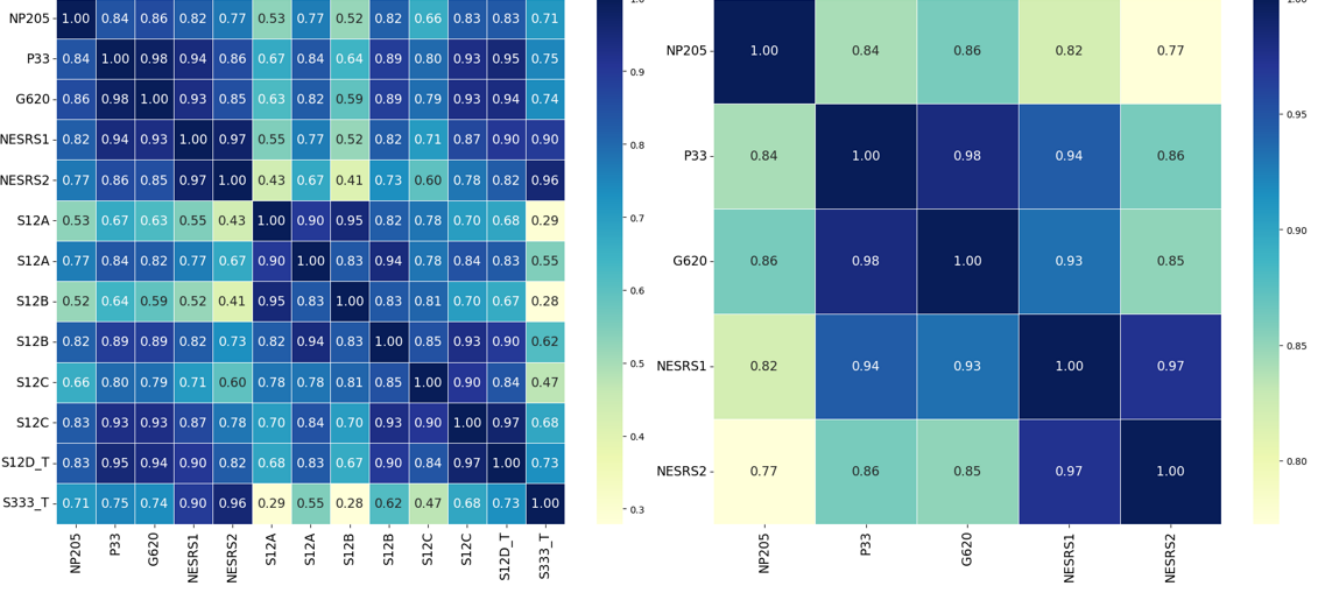


Figure 7: Correlation Analysis of water levels at five measuring water stations and nearby gates.

C More experimental results

Models	Lead Time	NP205		P33		G620		NESRS1		NESRS2		Overall	
		MAE	RMSE	MAE	RMSE	MAE	RMSE	MAE	RMSE	MAE	RMSE	MAE	RMSE
Sim-RAF (Strategy A)	7	0.117	0.206	0.056	0.104	0.069	0.127	0.063	0.115	0.057	0.107	0.072	0.132
	14	0.191	0.330	0.090	0.151	0.103	0.182	0.094	0.161	0.088	0.156	0.113	0.196
	21	0.251	0.425	0.118	0.189	0.139	0.232	0.126	0.201	0.118	0.197	0.151	0.249
	28	0.320	0.519	0.145	0.227	0.175	0.283	0.150	0.232	0.139	0.224	0.186	0.297
MI-RAF (Strategy A)	7	0.123	0.214	0.057	0.106	0.069	0.130	0.063	0.119	0.059	0.112	0.074	0.136
	14	0.184	0.324	0.087	0.151	0.102	0.183	0.092	0.162	0.086	0.158	0.110	0.195
	21	0.247	0.426	0.115	0.187	0.134	0.230	0.120	0.200	0.112	0.195	0.146	0.248
	28	0.304	0.519	0.141	0.226	0.172	0.281	0.142	0.231	0.132	0.225	0.178	0.295
Sim-RAF (Strategy C)	7	0.126	0.221	0.058	0.106	0.068	0.126	0.064	0.117	0.059	0.109	0.075	0.135
	14	0.204	0.335	0.093	0.152	0.110	0.180	0.098	0.164	0.090	0.160	0.119	0.198
	21	0.269	0.426	0.118	0.179	0.152	0.228	0.124	0.190	0.119	0.195	0.157	0.246
	28	0.330	0.500	0.142	0.209	0.175	0.265	0.154	0.226	0.149	0.228	0.190	0.290
MI-RAF (Strategy C)	7	0.118	0.218	0.054	0.104	0.063	0.124	0.059	0.115	0.054	0.108	0.070	0.133
	14	0.184	0.326	0.085	0.147	0.097	0.175	0.087	0.157	0.082	0.156	0.107	0.193
	21	0.237	0.408	0.111	0.177	0.128	0.214	0.114	0.191	0.106	0.188	0.139	0.236
	28	0.310	0.526	0.137	0.214	0.162	0.259	0.137	0.223	0.128	0.221	0.175	0.289

Table 5: Performance across 5 stations (NP205, P33, G620, NESRS1, NESRS2) for lead times of 7, 14, 21, and 28 days. The four models are our RAF methods with similarity-based and mutual information-based implementations utilizing the Strategy A and Strategy C techniques as mentioned in Section 2.3.

D More Visualizations

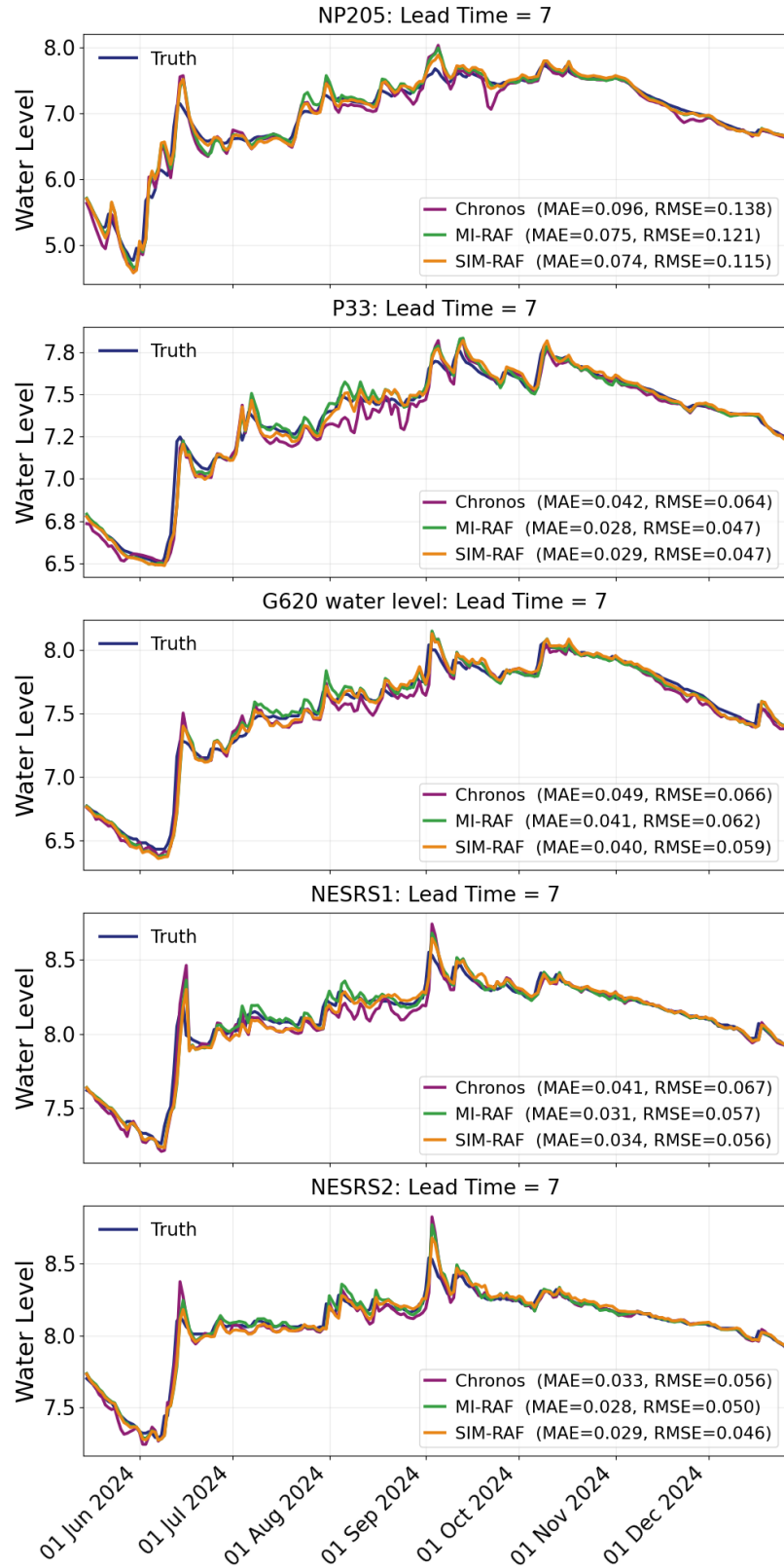


Figure 8: Visualization of true and predicted water levels for 7 days lead time.

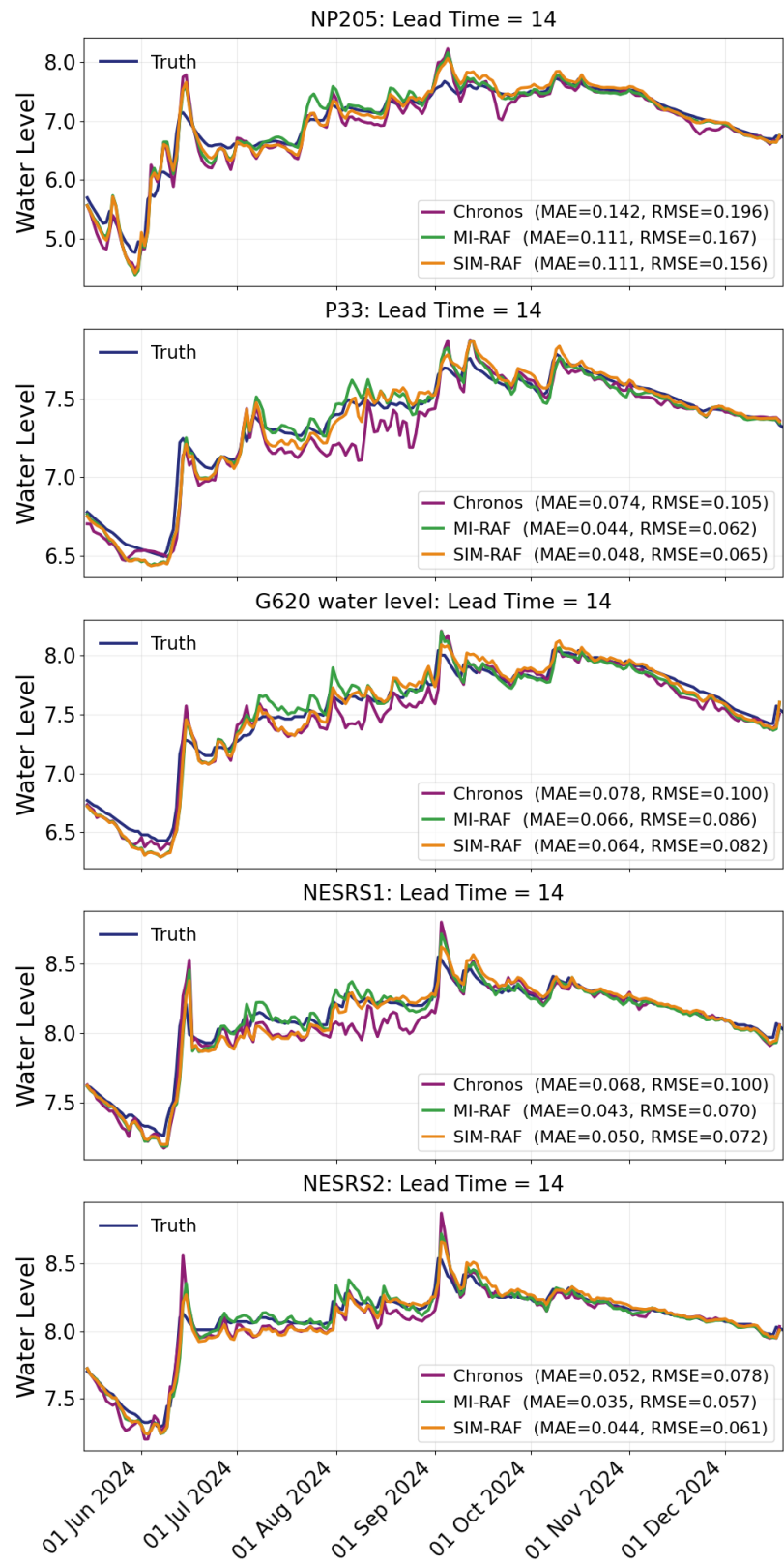


Figure 9: Visualization of true and predicted water levels for 14 days lead time.

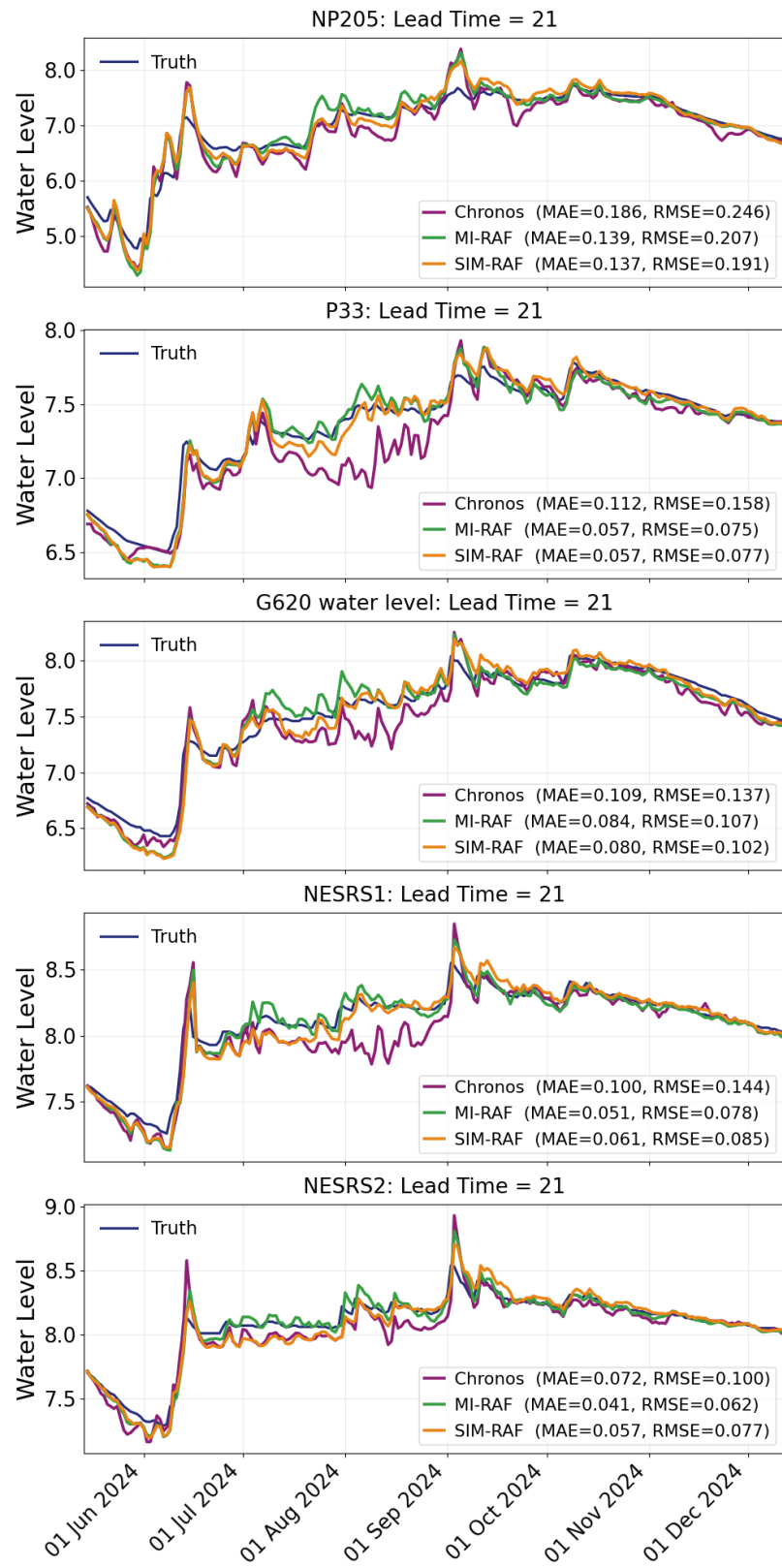


Figure 10: Visualization of true and predicted water levels for 21 days lead time.